

Structured Latent Dynamics in Wireless CSI via Homomorphic World Models

Salmane Naoumi[‡], Mehdi Bennis[†], and Marwa Chafii^{*‡}

^{*}Engineering Division, New York University (NYU), Abu Dhabi, UAE.

[†]Center for Wireless Communications, University of Oulu, Finland.

[‡]NYU WIRELESS, NYU Tandon School of Engineering, New York, USA.

Abstract—We introduce a self-supervised framework for learning predictive and structured representations of wireless channels by modeling the temporal evolution of channel state information (CSI) in a compact latent space. Our method casts the problem as a world modeling task and leverages the Joint Embedding Predictive Architecture (JEPA) to learn action-conditioned latent dynamics from CSI trajectories. To promote geometric consistency and compositionality, we parameterize transitions using homomorphic updates derived from Lie algebra, yielding a structured latent space that reflects spatial layout and user motion. Evaluations on the DICHASUS dataset show that our approach outperforms strong baselines in preserving topology and forecasting future embeddings across unseen environments. The resulting latent space enables metrically faithful channel charts, offering a scalable foundation for downstream applications such as mobility-aware scheduling, localization, and wireless scene understanding.

Index Terms—Predictive world models, Channel Charting, Wireless Representation Learning, Self-Supervised Learning, Joint Embedding Predictive Architecture.

I. INTRODUCTION

World models (WMs) have emerged as a powerful paradigm in artificial intelligence (AI), enabling agents to internalize environmental dynamics and simulate future states rather than react solely to immediate observations. At their core, WMs construct compact latent representations of the world and leverage them to predict the consequences of actions, reason about outcomes, and guide decision-making under uncertainty. Foundational works, such as that of Ha and Schmidhuber [1], demonstrated how compressing high-dimensional sensory inputs into a latent space enables agents to plan and act more efficiently. More recent frameworks, including Joint-Embedding Predictive Architectures (JEPAs) [2], shift focus to predicting hidden or future representations directly in latent space, offering a self-supervised path toward learning causal and temporally coherent abstractions. Such models support internal simulations that enhance long-horizon reasoning, counterfactual inference, and policy planning [3], [4].

Integrating WMs into wireless communication systems offers a promising route toward autonomous and adaptive network intelligence [5]. Wireless environments pose unique challenges: observations (e.g., channel state information (CSI)) are high-dimensional and noisy, channel dynamics are governed by complex physical processes, and real-time constraints demand low-latency, safe decision-making. Embedding a WM within a wireless agent can help anticipate future channel

states, evaluate strategies before deployment, and generalize to unseen conditions. Recent works such as Wireless Dreamer [6] and MobiWorld [7] illustrate how world models embedded in edge agents enable simulation-based efficient planning, improved generalization, and robust policy optimization.

While prior efforts have focused on leveraging WMs for wireless control and decision-making, an open question remains: can the latent space of a WM also serve as a meaningful representation of the radio environment? Channel charting (CC) addresses a related goal by embedding high-dimensional CSI into a lower dimensional latent space that preserves spatial proximity [8]. Classical approaches rely on handcrafted dissimilarity metrics derived from angular or delay domain features and apply manifold learning or Siamese contrastive training [9]. However, these methods are typically static, lack temporal awareness, and require domain-specific priors.

In this work, we build upon recent advances in predictive representation learning for wireless channels, particularly the JEPA-based formulation of [10], which conditions on user velocity to forecast future channel embeddings. While effective, their method follows a two-stage curriculum, first pretraining a conventional CC model and then learning dynamics atop that representation. By contrast, we propose a unified, self-supervised predictive WM trained end-to-end from raw CSI sequences without intermediate supervision. Our architecture follows the JEPA formulation [11], [12], augmented with action conditioning and structured latent transitions inspired by recent advances in equivariant representation learning [13]. A key novelty lies in our introduction of homomorphic latent dynamics: instead of treating latent transitions as generic mappings, we enforce compositional structure by learning action representations that operate as smooth and consistent transformations in latent space. This approach enables the model to predict the outcomes of arbitrary action sequences with high geometric fidelity, without requiring prior knowledge of the transformation group or restrictions on the action space. As a result, our model constructs a predictive CC, a latent geometry that not only captures spatial structure but also supports temporally coherent rollouts.

In summary, our contributions are as follows:

- We propose a self-supervised predictive WM for wireless channel modeling, trained on temporally coherent CSI trajectories and equipped with action-conditioned latent transitions.

- We introduce a homomorphic transition operator based on Lie algebra parameterizations and matrix exponentials, enabling structured and compositional dynamics in the latent space. To the best of our knowledge, this is the first application of homomorphic latent JEPA-style architectures to radio channel modeling.
- We show that the learned encoder functions as a forward charting function (FCF), mapping CSI into a metrically faithful latent space. We quantitatively evaluate the resulting predictive CC using standard metrics such as trustworthiness (TW), continuity (CT), kruskal’s stress (KS), and rajski’s distance (RD).
- We conduct extensive experiments on the DICHASUS dataset, demonstrating that our model outperforms strong baselines including multi-layer perceptron (MLP), gated recurrent unit (GRU), and feature-wise linear modulation (FiLM) predictors, and generalizes effectively to unseen environments without retraining.

II. SYSTEM MODEL

We consider a wireless sensing setting in which a single-antenna user equipment (UE) communicates with B spatially distributed base stations (BSs), each equipped with an M -element antenna array. The UE transmits an orthogonal frequency-division multiplexing (OFDM) waveform over N_{sub} subcarriers. At each discrete time step t , all BSs synchronously record the downlink CSI in the frequency domain, resulting in a wideband multi-antenna tensor $\mathbf{H}_t^{(n)} \in \mathbb{C}^{B \times M \times N_{\text{sub}}}$, where $\mathbf{H}_t^{(n)}$ denotes the CSI observed at time t in trajectory n . Each CSI snapshot is paired with a timestamp $t_t^{(n)} \in \mathbb{R}$ and a ground-truth user position $\mathbf{x}_t^{(n)} \in \mathbb{R}^3$, yielding a sequence of spatial-temporal observations

$$\mathcal{S} = \left\{ \left(\mathbf{H}_t^{(n)}, \mathbf{x}_t^{(n)}, t_t^{(n)} \right) \right\}_{t=0}^{T_n}, \quad n = 1, \dots, N,$$

where T_n is the number of snapshots in the n^{th} trajectory. To model the temporal dynamics of channel evolution, we augment each trajectory with control inputs reflecting the UE’s motion. Specifically, we define the control vector $\mathbf{a}_t^{(n)} \in \mathbb{R}^d$ as a 2D velocity signal estimated from consecutive positions. This yields a temporally ordered trajectory with control annotations of the form

$$\mathcal{D} = \left\{ \tau^{(n)} = \left(\mathbf{H}_0^{(n)}, \mathbf{a}_0^{(n)}, \mathbf{H}_1^{(n)}, \dots, \mathbf{a}_{T_n-1}^{(n)}, \mathbf{H}_{T_n}^{(n)} \right) \right\}_{n=1}^N. \quad (1)$$

The velocity based inputs $\mathbf{a}_t^{(n)}$ act as action-like signals governing state transitions, allowing us to interpret the dataset as a sequence of interactions from an underlying dynamical system.

This structure lends itself naturally to a Markov Decision Process (MDP) abstraction, defined as $\mathcal{M} = (\mathcal{S}, \mathcal{A}, \mu, p)$, where \mathcal{S} is the state space of CSI observations, $\mathcal{A} \subset \mathbb{R}^d$ is the control (or action) space, μ is the initial state distribution, and $p(\mathbf{H}_{t+1} | \mathbf{H}_t, \mathbf{a}_t)$ defines the stochastic transition dynamics driven by motion. Although no reward signals are defined in this setup, the MDP structure enables the learning

of predictive models of channel evolution without explicit supervision, thereby supporting a wide range of downstream wireless applications such as beam tracking, mobility-aware scheduling, and proactive resource management. As detailed in Section III, we propose to learn such models via structured latent representations, without relying on spatial labels or handcrafted similarity metrics.

III. PROPOSED SOLUTION

In contrast to traditional manifold learning and metric-based CC techniques that rely on pairwise dissimilarities, we propose a structured WM framework to learn predictive, geometry-aware latent representations of multi-antenna wideband CSI. As illustrated in Figure 1, we treat the evolution of the wireless channel as a latent dynamical system driven by user motion, modeled as control-conditioned transitions in latent space. We assume that the wireless environment remains predominantly static over the duration of each trajectory, i.e., the spatial layout of reflectors and scatterers is fixed and no abrupt occlusions occur. Hence, we model the dynamics of the observed channel as primarily governed by user motion. While small-scale effects and noise may contribute to variability, we assume these manifest as temporally smooth and locally continuous deviations. Accordingly, we take the UE’s 2D velocity as the primary control signal driving state transitions. Under this abstraction, the model learns a compact latent representation $\mathbf{z}_t = \zeta(\tilde{\mathbf{H}}_t) \in \mathbb{R}^D$ from a preprocessed CSI tensor $\tilde{\mathbf{H}}_t$, and a transition operator ψ such that

$$\hat{\mathbf{z}}_{t+h} = \psi(\mathbf{z}_t; \mathbf{a}_t, \dots, \mathbf{a}_{t+h-1}), \quad (2)$$

enabling structured prediction of future embeddings based on sequences of the UE motion.

Each complex CSI observation $\mathbf{H}_t^{(n)} \in \mathbb{C}^{B \times M \times N_{\text{sub}}}$ is transformed into a real-valued tensor $\tilde{\mathbf{H}}_t^{(n)} \in \mathbb{R}^{2 \times (B \cdot M) \times N_{\text{sub}}}$ by concatenating magnitude and phase. These are processed by a shared encoder $\zeta = h_\theta$, yielding latent embeddings $\mathbf{z}_t^{(n)} = h_\theta(\tilde{\mathbf{H}}_t^{(n)}) \in \mathbb{R}^D$. During training, we extract sub-sequences of length $H + 1$ from each trajectory, along with H associated control vectors

$$\tau_t^{(n)} = \left(\tilde{\mathbf{H}}_t^{(n)}, \mathbf{a}_t^{(n)}, \tilde{\mathbf{H}}_{t+1}^{(n)}, \dots, \mathbf{a}_{t+H-1}^{(n)}, \tilde{\mathbf{H}}_{t+H}^{(n)} \right). \quad (3)$$

In predictive representation learning, prior work such as PLDM [12] models latent dynamics using a generic transition function f_Θ implemented as a generic neural network (NN)

$$\hat{\mathbf{z}}_{t+h} = f_\Theta(\mathbf{z}_t, \mathbf{a}_t, \dots, \mathbf{a}_{t+h-1}). \quad (4)$$

However, such mappings are often unstructured, limiting generalization across varying motion patterns. Instead, we propose a structured dynamics model inspired by [13], where control inputs induce transformations in the latent space via compositions of Lie group actions. Specifically, we define a learnable mapping $\phi_\Theta : \mathbb{R}^d \rightarrow \mathfrak{gl}(D)$ that projects control inputs \mathbf{a}_t into a Lie algebra. The corresponding Lie group element is then obtained via the matrix exponential

$$\rho_\Theta(\mathbf{a}_t) = \exp(\phi_\Theta(\mathbf{a}_t)). \quad (5)$$

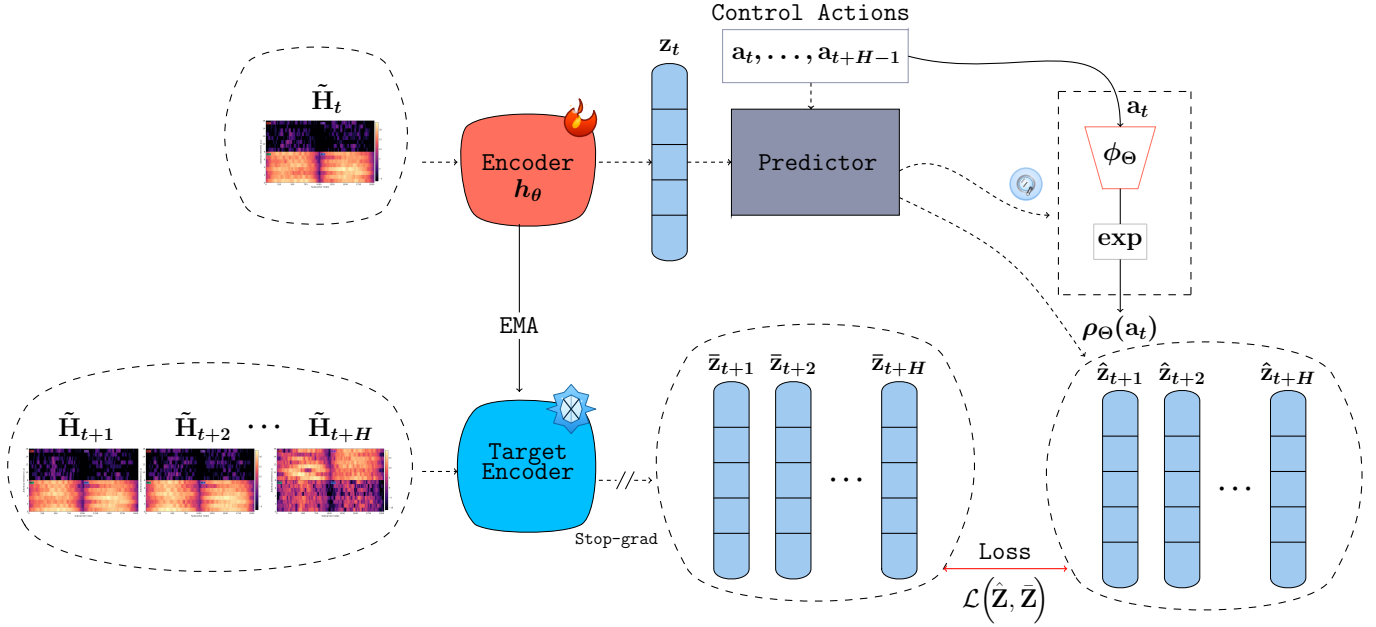


Fig. 1: Overview of the proposed WM architecture. The model encodes real-valued CSI tensors into latent vectors, then evolves them through a structured, Lie group-based transition model conditioned on user motion. It is trained via self-supervised rollout prediction and regularized to preserve geometric consistency and action-awareness.

Future latents are then predicted via successive group compositions acting on the current state

$$\hat{\mathbf{z}}_{t+h} = \left(\prod_{i=0}^{h-1} \rho_{\Theta}(\mathbf{a}_{t+i}) \right) \mathbf{z}_t. \quad (6)$$

This homomorphic structure ensures temporal consistency, algebraic compositionality, and geometric coherence in the latent dynamics.

We train our model using a self-supervised predictive objective that encourages consistent latent rollouts across temporally aligned channel observations. Drawing inspiration from JEPAs [11], [12], the training framework adopts a teacher-student setup wherein the model is optimized to forecast future representations under action-conditioned latent dynamics. The encoder h_{θ} generates online embeddings \mathbf{z}_t , while a non-trainable target encoder h_{EMA} is maintained as an exponential moving average (EMA) of the online encoder and produces reference embeddings $\bar{\mathbf{z}}_{t+h} = h_{\text{EMA}}(\tilde{\mathbf{H}}_{t+h})$ for each future step $t+h$. The predicted latent $\hat{\mathbf{z}}_{t+h}$ is computed via Eq. (6) using the online encoder and control sequence.

To train the latent predictor, we extract rollout segments of horizon H from each trajectory, organizing them into batches of size K . Let $\hat{\mathbf{Z}}, \bar{\mathbf{Z}} \in \mathbb{R}^{H \times K \times D}$ represent the predicted and target latent sequences, respectively. We begin by minimizing a teacher-forcing loss, aligning each predicted latent to its corresponding target using an ℓ_1 loss

$$\mathcal{L}_{\text{TF}} = \frac{1}{HK} \sum_{t=1}^H \sum_{b=1}^K \left\| \hat{\mathbf{z}}_{t,b} - \bar{\mathbf{z}}_{t,b} \right\|_1. \quad (7)$$

To promote consistency over the full prediction horizon, we include an additional rollout loss that supervises only the terminal latent

$$\mathcal{L}_{\text{roll}} = \frac{1}{K} \sum_{b=1}^K \left\| \hat{\mathbf{z}}_{H,b} - \bar{\mathbf{z}}_{H,b} \right\|_1. \quad (8)$$

While these losses encourage local alignment, they do not explicitly regularize the structure of the latent space. To address this, we incorporate a VICReg-style regularization [14], which encourages non-degenerate and decorrelated embeddings. The variance term ensures that each latent dimension maintains sufficient spread across the batch

$$\mathcal{L}_{\text{var}} = \frac{1}{HD} \sum_{t=1}^H \sum_{j=1}^D \max \left(0, \gamma - \sqrt{\text{Var}(\bar{\mathbf{z}}_{t,:,j}) + \epsilon} \right), \quad (9)$$

where γ is a target standard deviation hyperparameter and ϵ is a small constant introduced to ensure numerical stability. Additionally, we apply a covariance penalty that reduces linear correlations among embedding dimensions using the empirical covariance matrix.

$$C(\bar{\mathbf{Z}}_t) = \frac{1}{K-1} (\bar{\mathbf{Z}}_t - \bar{\bar{\mathbf{Z}}}_t)^\top (\bar{\mathbf{Z}}_t - \bar{\bar{\mathbf{Z}}}_t), \quad (10)$$

$$\mathcal{L}_{\text{cov}} = \frac{1}{HD} \sum_{t=1}^H \sum_{i \neq j} [C(\bar{\mathbf{Z}}_t)]_{i,j}^2, \quad (11)$$

where $\bar{\bar{\mathbf{Z}}}_t = \frac{1}{K} \sum_{b=1}^K \bar{\mathbf{z}}_{t,b}$ denotes the batch mean at time t .

To further reinforce the action-aware structure of the learned embeddings, we introduce an inverse dynamics modeling (IDM) loss [15]. A frozen MLP g_{ψ} , initialized at the beginning

of training, is tasked with decoding the control input from consecutive latent pairs. This encourages the learned representations to contain information predictive of motion

$$\mathcal{L}_{\text{IDM}} = \frac{1}{HK} \sum_{t=1}^H \sum_{b=1}^K \|\mathbf{a}_{t-1,b} - g_\psi(\bar{\mathbf{Z}}_{t-1,b}, \bar{\mathbf{Z}}_{t,b})\|_2^2. \quad (12)$$

The final training objective aggregates all losses into a weighted sum

$$\mathcal{L}_{\text{total}} = \lambda_{\text{TF}} \mathcal{L}_{\text{TF}} + \lambda_{\text{roll}} \mathcal{L}_{\text{roll}} + \lambda_{\text{var}} \mathcal{L}_{\text{var}} + \lambda_{\text{cov}} \mathcal{L}_{\text{cov}} + \lambda_{\text{IDM}} \mathcal{L}_{\text{IDM}}, \quad (13)$$

where we use default values $\lambda_{\text{TF}} = 1.0$, $\lambda_{\text{roll}} = 2.0$, $\lambda_{\text{var}} = 2.0$, $\lambda_{\text{cov}} = 10.0$, and $\lambda_{\text{IDM}} = 1.0$. These weights were selected via hyperparameter search on a held-out validation set and fixed across all experiments, unless stated otherwise.

Model training is conducted for 100 epochs using the AdamW optimizer. The learning rate follows a cosine decay schedule with a 5% linear warm-up, starting at 10^{-4} , peaking at 3×10^{-4} , and decaying to 10^{-6} . Weight decay is linearly ramped from 0.04 to 0.4 across training. A batch size of 128 is used throughout, and the EMA target encoder is updated with a decay factor of 0.9995 to ensure smooth representation drift. This training setup enables the model to learn temporally predictive, geometrically structured, and action-consistent embeddings that support robust rollout forecasting and trajectory unfolding in wireless environments.

IV. NUMERICAL EVALUATION

We evaluate our approach on the DICHASUS dataset [16], which contains wideband indoor channel measurements acquired by a distributed channel sounder. The setup consists of a single antenna transmitter mounted on a mobile robot and $B = 4$ spatially distributed receiver arrays, each equipped with $M = 8$ antennas arranged in a 2×4 configuration, for a total of 32 receive antennas. The system operates over $N_{\text{sub}} = 1024$ OFDM subcarriers spanning a 50 MHz bandwidth centered at 1.272 GHz, with CSI snapshots recorded every 40 ms. Each sample includes a complex valued frequency domain CSI tensor $\mathbf{H} \in \mathbb{C}^{B \times M \times N_{\text{sub}}}$ alongside ground truth positions and timestamps. To reduce input dimensionality while retaining essential channel structure, we apply a time domain truncation that compresses the number of subcarriers to 64. The resulting tensor is cast into a two channel real-valued representation containing the magnitude and wrapped phase of the complex coefficients, yielding inputs of shape $(2, 32, 64)$. We use subsets cf02, cf03, and cf07 for training, totaling 25,149 samples, and evaluate on cf04, cf05, and cf06. While all subsets are recorded in the same L-shaped industrial space, they contain distinct motion paths, allowing us to assess generalization to novel trajectories. The CSI samples are segmented into temporally coherent trajectories, as described in Section III, for sequential modeling.

The encoder h_θ is a ResNet-style convolutional network [17], with four stages of depths [3, 4, 6, 3] and channel dimensions [128, 192, 256, 256], each followed by downsampling. GeLU activations and BatchNorm are used throughout.

The output is pooled and normalized to obtain a $D = 128$ -dimensional latent embedding, which we found to offer the best balance between training stability and charting quality across validation subsets. The dynamics model ϕ_Θ is a two-layer MLP with GeLU activations, mapping control inputs to $D \times D$ matrix generators, which are exponentiated to yield linear operators in the latent space. The IDM module g_ψ is a frozen two-layer MLP with ReLU activations. We use a rollout horizon $H = 6$ and tube masking ratio $r_m = 0.15$.

The proposed architecture serves a predictive WM trained on temporally coherent CSI trajectories. We posit that the encoder, once trained, functions as a FCF, projecting high-dimensional CSI observations into a compact latent space wherein euclidean distances correlate with spatial displacements between the UE positions. To quantify this behavior, we report four metrics from the channel charting literature: CT, TW, KS, and RD. CT and TW are optimal at 1 and measure local structure preservation, while KS and RD are optimal at 0 and reflect the global topological alignment.

Figure 2 visualizes predicted latent rollouts on representative training and test trajectories. Starting from an initial CSI input, the model generates future embeddings conditioned solely on velocity sequences, without access to future CSIs. The resulting latent trajectories, visualized using principal component analysis (PCA), preserve both temporal coherence and geometric structure, closely matching the ground truth positions even in unseen environments. The third row shows aligned projections via Procrustes analysis for spatial interpretability.

Table I compares the proposed homomorphic transition model to baseline predictors trained under the same losses. The MLP baseline models dynamics as an unconstrained function of (z_t, a_t) . FiLM [18] introduces action-dependent affine modulation

$$z_{t+1} = z_t + \gamma(a_t) \odot z_t + \beta(a_t), \quad (14)$$

where $\gamma(a_t), \beta(a_t) \in \mathbb{R}^D$ are learned via MLPs. The GRU predictor adopts a recurrent architecture as in [10]. Our method enforces compositional latent transitions via homomorphic mappings $\exp(\phi_\Theta(a_t))$, promoting algebraic structure and smoothness across action sequences. The proposed method consistently outperforms all baselines across metrics, demonstrating that enforcing homomorphic latent transitions yields more structured and metrically faithful embeddings. Notably, our model generalizes to test trajectories never seen during training, highlighting the benefit of compositional structure for predictive and generalizable channel charting.

To evaluate the contribution of the individual loss components, we conduct an ablation study summarized in Table II. Removing both VICReg and IDM regularization (Teacher-forcing + Rollout loss only) leads to a pronounced drop in performance, with reduced local structure (CT = 0.6443) and degraded global alignment (RD = 0.9719). Adding VICReg alone improves both TW and CT, demonstrating the importance of embedding regularization. Replacing VICReg with a predictive loss maintains moderate structure but yields

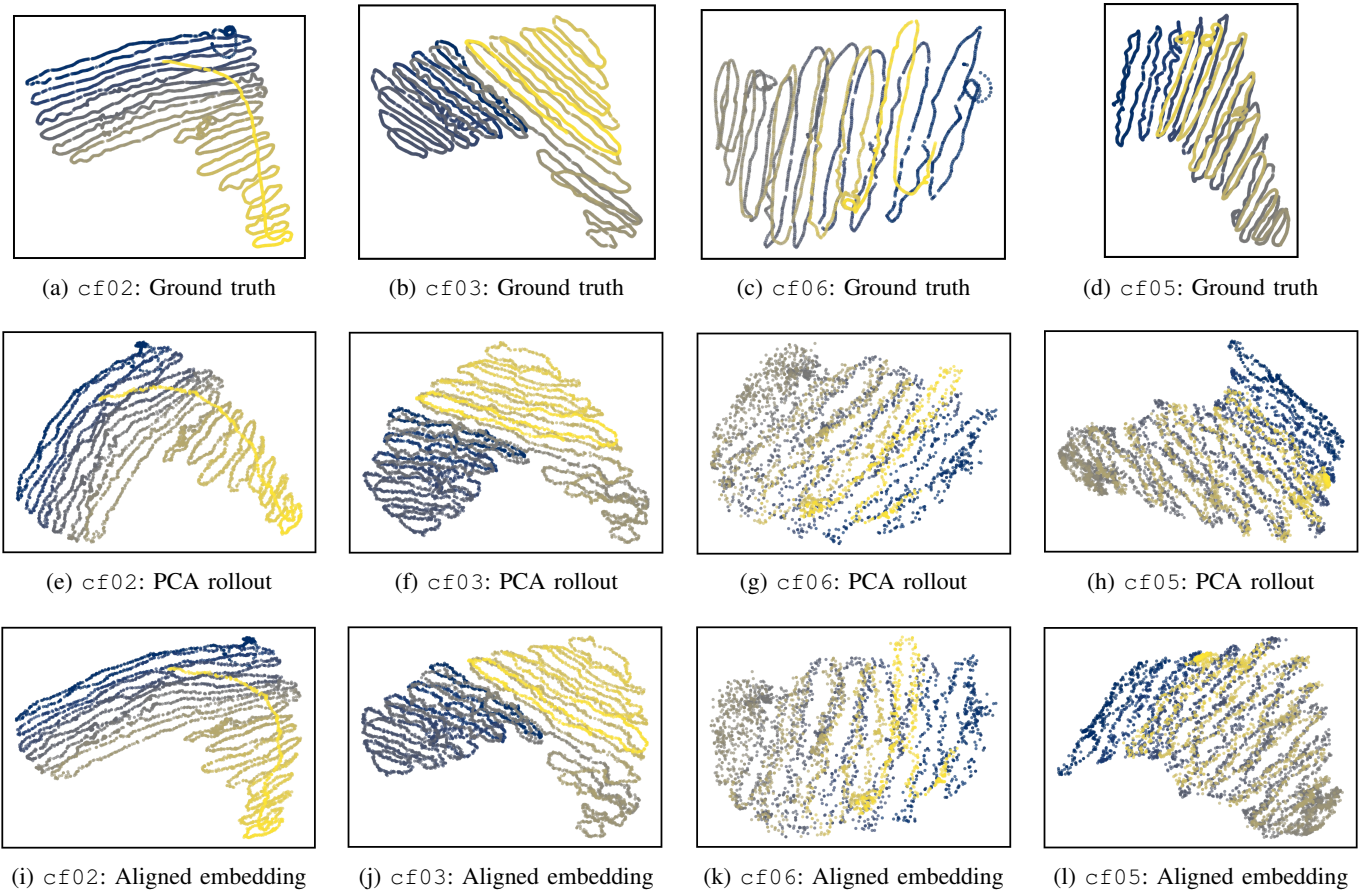


Fig. 2: **Visualization of latent rollouts vs. ground truth trajectories.** Each column corresponds to a scene (cf02, cf03, cf06, cf05). Top row: Ground truth user trajectories in physical space. Middle row: PCA projections of predicted latent rollouts using the trained model and input velocity sequences. Bottom row: Same latent rollouts, aligned (via Procrustes) to the ground-truth positions. The learned latent space exhibits spatial and temporal consistency across both seen and unseen environments.

Predictor	\uparrow TW	\uparrow CT	\downarrow KS	\downarrow RD
Proposed	0.9948 \pm 0.0026	0.9764 \pm 0.0178	0.1001 \pm 0.0351	0.7473 \pm 0.0758
FiLM	0.9935 \pm 0.0033	0.9640 \pm 0.0273	0.1330 \pm 0.0488	0.8149 \pm 0.0680
MLP	0.9927 \pm 0.0029	0.9622 \pm 0.0168	0.1234 \pm 0.0354	0.7828 \pm 0.0667
GRU	0.9916 \pm 0.0039	0.9680 \pm 0.0170	0.1190 \pm 0.0340	0.7818 \pm 0.0571

TABLE I: **Chart quality metrics on held-out subsets (cf04, cf05, cf06).** Mean \pm standard deviation across trajectories. Higher is better for TW, CT; lower is better for KS, RD.

Loss Components	TW \uparrow	CT \uparrow	KS \downarrow	RD \downarrow
TF + Roll + VICReg + IDM	0.9996	0.9994	0.0388	0.6057
TF + Roll + IDM	0.9988	0.9934	0.0629	0.6605
TF + Roll + VICReg	0.9984	0.9986	0.0640	0.7326
TF + Roll	0.9760	0.6443	0.5593	0.9719

TABLE II: **Ablation of loss components on latent chart quality.** Results are reported for the testing sets using standard metrics. Adding VICReg and IDM regularization significantly improves both local and global structure.

higher distortion. The best performance is achieved when both VICReg and IDM are included, suggesting that variance decorrelation and motion-aware supervision jointly encourage temporally stable and metrically faithful representations. These findings highlight the complementary role of information-theoretic and dynamics-aware objectives in structuring the latent space.

Finally, while our evaluation primarily focuses on geometric fidelity and rollout consistency of the learned latent space, we note that downstream applications such as beam selection, handover prediction, or user scheduling can be naturally built

atop the proposed representation. However, such tasks typically require additional domain-specific components, labels, or control policies, which fall outside the core scope of this work. Our goal is to establish the predictive and compositional structure of the latent dynamics, which we consider a necessary precursor to reliable downstream reasoning. As a first step, we assume a predominantly static environment where channel evolution is governed by user motion. Extending this framework to handle dynamic settings with time-varying scatterers, non-line-of-sight conditions, or multipath variability is critical for real-world deployment. Moreover, incorporating constraints on computational efficiency such as latency, memory footprint, or FLOPs will be essential for enabling integration into latency-sensitive wireless pipelines. We leave both robustness and system-level optimization as promising directions for future work.

V. CONCLUSION

In this work, we proposed a predictive world modeling framework tailored to wireless environments, leveraging the temporal structure of evolving CSI measurements. By recasting channel charting as a latent dynamics learning problem, we introduced a self-supervised architecture based on JEPa that learns action-conditioned transitions in a compact latent space. To enforce geometric consistency and compositionality, we incorporated homomorphic updates via Lie algebraic parameterizations, yielding a structured transition model capable of stable and interpretable rollouts. Our experiments on the DICHASUS dataset demonstrate that the learned latent space preserves spatial topology and generalizes across diverse motion trajectories. These findings suggest that predictive WMs offer a principled foundation for constructing geometry-aware wireless representations. Future work will investigate the integration of this approach into end-to-end systems for downstream tasks such as localization, adaptive beamforming, and autonomous wireless decision-making.

ACKNOWLEDGMENT

This work was supported in part by the NYU Abu Dhabi Center for Artificial Intelligence and Robotics, funded by Tamkeen under the Research Institute Award CG010, and by the Technology Innovation Institute (TII). The authors also acknowledge use of the High Performance Computing resources at New York University Abu Dhabi.

REFERENCES

- [1] D. Ha and J. Schmidhuber, "Recurrent world models facilitate policy evolution," in *Advances in Neural Information Processing Systems 31*, pp. 2451–2463, Curran Associates, Inc., 2018.
- [2] Y. LeCun and Courant, "A path towards autonomous machine intelligence version 0.9.2, 2022-06-27," 2022.
- [3] Z. Zhu, X. Wang, W. Zhao, C. Min, N. Deng, M. Dou, Y. Wang, B. Shi, K. Wang, C. Zhang, Y. You, Z. Zhang, D. Zhao, L. Xiao, J. Zhao, J. Lu, and G. Huang, "Is sora a world simulator? a comprehensive survey on general world models and beyond," *arXiv preprint arXiv:2405.03520*, 2024.
- [4] J. Ding, Y. Zhang, Y. Shang, Y. Zhang, Z. Zong, J. Feng, Y. Yuan, H. Su, N. Li, N. Sukiennik, F. Xu, and Y. Li, "Understanding world or predicting future? a comprehensive survey of world models," *ACM Comput. Surv.*, vol. 58, Sept. 2025.

- [5] W. Saad, O. Hashash, C. K. Thomas, C. Chaccour, M. Debbah, N. Mandayam, and Z. Han, "Artificial general intelligence (AGI)-native wireless systems: A journey beyond 6G," *Proceedings of the IEEE*, pp. 1–39, 2025.
- [6] C. Zhao, R. Zhang, J. Wang, G. Zhao, D. Niyato, G. Sun, S. Mao, and D. I. Kim, "World models for cognitive agents: Transforming edge intelligence in future networks," 2025.
- [7] H. Chai, Y. Yuan, and Y. Li, "Mobiworld: World models for mobile wireless network," 2025.
- [8] C. Studer, S. Medjkouh, E. Gonultaş, T. Goldstein, and O. Tirkkonen, "Channel charting: Locating users within the radio environment using channel state information," *IEEE Access*, vol. 6, pp. 47682–47698, 2018.
- [9] P. Stephan, F. Euchner, and S. t. Brink, "Angle-delay profile-based and timestamp-aided dissimilarity metrics for channel charting," *IEEE Transactions on Communications*, vol. 72, no. 9, pp. 5611–5625, 2024.
- [10] C. Bou Chaaya, A. M. Girgis, and M. Bennis, "Learning latent wireless dynamics from channel state information," *IEEE Wireless Communications Letters*, vol. 14, no. 2, pp. 489–493, 2025.
- [11] M. Assran, A. Bardes, D. Fan, Q. Garrido, R. Howes, M. Komeili, M. Muckley, A. Rizvi, C. Roberts, K. Sinha, A. Zholus, S. Arnaud, A. Gejji, A. Martin, F. Robert Hogan, D. Dugas, P. Bojanowski, V. Khaldov, P. Labatut, F. Massa, M. Szafraniec, K. Krishnakumar, Y. Li, X. Ma, S. Chandar, F. Meier, Y. LeCun, M. Rabbat, and N. Ballas, "V-jepa 2: Self-supervised video models enable understanding, prediction and planning," *arXiv preprint arXiv:2506.09985*, 2025.
- [12] V. Sobal, W. Zhang, K. Cho, R. Balestrieri, T. G. J. Rudner, and Y. LeCun, "Learning from reward-free offline data: A case for planning with latent dynamics models," *arXiv preprint arXiv:2502.14819*, 2025.
- [13] H. Keurti, H.-R. Pan, M. Besserve, B. Grewe, and B. Schölkopf, "Homomorphism autoencoder—learning group structured representations from observed transitions," in *Proceedings of the 40th International Conference on Machine Learning, ICMML'23*, JMLR.org, 2023.
- [14] A. Bardes, J. Ponce, and Y. LeCun, "Vicreg: Variance-invariance-covariance regularization for self-supervised learning," *CoRR*, vol. abs/2105.04906, 2021.
- [15] T. Lesort, N. Díaz-Rodríguez, J.-F. Goudou, and D. Filliat, "State representation learning for control: An overview," *Neural Networks*, vol. 108, pp. 379–392, 2018.
- [16] F. Euchner and M. Gauger, "CSI Dataset dichasus-cf0x: Distributed Antenna Setup in Industrial Environment, Day 1," 2022.
- [17] K. He, X. Zhang, S. Ren, and J. Sun, "Deep Residual Learning for Image Recognition," in *Proceedings of 2016 IEEE Conference on Computer Vision and Pattern Recognition, CVPR '16*, pp. 770–778, IEEE, June 2016.
- [18] E. Perez, F. Strub, H. de Vries, V. Dumoulin, and A. C. Courville, "Film: Visual reasoning with a general conditioning layer," in *AAAI*, 2018.